

# The edge of awareness: Mask spatial density, but not color, determines optimal temporal frequency for continuous flash suppression

[Jan Drewes](#); [Weina Zhu](#); [David Melcher](#)

+ Author Affiliations & Notes

Journal of Vision January 2018, Vol.18, 12. doi:10.1167/18.1.12

## Abstract

The study of how visual processing functions in the absence of visual awareness has become a major research interest in the vision-science community. One of the main sources of evidence that stimuli that do not reach conscious awareness—and are thus “invisible”—are still processed to some degree by the visual system comes from studies using continuous flash suppression (CFS). Why and how CFS works may provide more general insight into how stimuli access awareness. As spatial and temporal properties of stimuli are major determinants of visual perception, we hypothesized that these properties of the CFS masks would be of significant importance to the achieved suppression depth. In previous studies however, the spatial and temporal properties of the masks themselves have received little study, and masking parameters vary widely across studies, making a metacomparison difficult. To investigate the factors that determine the effectiveness of CFS, we varied both the temporal frequency and the spatial density of Mondrian-style masks. We consistently found the longest suppression duration for a mask temporal frequency of around 6 Hz. In trials using masks with reduced spatial density, suppression was weaker and frequency tuning was less precise. In contrast, removing color reduced mask

effectiveness but did not change the pattern of suppression strength as a function of frequency. Overall, this pattern of results stresses the importance of CFS mask parameters and is consistent with the idea that CFS works by disrupting the spatiotemporal mechanisms that underlie conscious access to visual input.

## Introduction

The study of how visual processing functions in the absence of visual awareness has become a major research interest in the vision-science community. One of the main sources of evidence that stimuli that do not reach conscious awareness—and are thus “invisible”—are still processed to some degree by the visual system comes from studies using binocular rivalry (Levelt, [1965](#); Wheatstone, [1838](#)) or continuous flash suppression (CFS; Tsuchiya & Koch, [2005](#)). Both the extraction of low-level visual features—such as orientation (Montaser-Kouhsari, Moradi, Zandvakili, & Esteky, [2004](#); Tsuchiya & Koch, [2005](#)), spatial information (van Boxtel, Tsuchiya, & Koch, [2010](#)), and motion (Kaunitz, Fracasso, & Melcher, [2011](#))—and the binding of low-level visual features based on gestalt grouping cues, such as good continuation and proximity (Mitroff & Scholl, [2005](#)), have been reported to occur in the absence of awareness. It has also been reported that some effects generally attributed to high-level stages of visual processing may be possible without being aware of the percept—for example, in face inversion (Jiang, Costello, & He, [2007](#); Stein, Hebart, & Sterzer, [2011](#); Zhou, Zhang, Liu, Yang, & Qu, [2010](#)), face expressions (Jiang et al., [2009](#); Smith, [2012](#)), semantic information (Costello, Jiang, Baartman, McGlennen, & He, [2009](#); Jiang et al., [2007](#); Kang, Blake, & Woodman, [2011](#)), and information integration (Lin & He, [2009](#); Lin & Murray, [2014](#); Mudrik, Breska, Lamy, & Deouell, [2011](#)). In particular, CFS has become the most popular tool for investigating visual processing outside of conscious awareness, although the exact nature of some of these effects remains controversial (Moors, Hesselmann, Wagemans, & van Ee, [2017](#); Sterzer, Stein, Ludwig, Rothkirch, & Hesselmann, [2014](#); Yang, Brascamp, Kang, & Blake, [2014](#)).

In a typical CFS paradigm, a series of contour-rich, high-contrast masks called Mondrian patterns are continuously flashed to one eye at a steady rate (temporal frequency), causing a static low-contrast image presented to the other eye to be

reliably suppressed throughout a viewing period that is substantially longer than in conventional binocular rivalry (Tsuchiya & Koch, [2005](#); Tsuchiya, Koch, Gilroy, & Blake, [2006](#)). Unfortunately, many studies utilizing CFS do not specify in any detail how the masks were designed. The consensus seems to be that, somewhat resembling the artistic style of the well-known artist Pieter Cornelis Mondriaan (Mondrian), these masks are designed from a number of overlapping rectangles of different colors or luminances.

Temporal factors play a critical role in determining the effectiveness of CFS (Tsuchiya & Koch, [2005](#); Zhu, Drewes, & Melcher, [2016](#)). Interestingly, the optimal temporal frequency reported in these studies is relatively low, around 6 Hz, with lower or higher frequencies leading to less effective suppression. Another study compared CFS displays with either the high or the low temporal frequencies removed, and found that the high temporal-frequency range was less effective at producing strong suppression (Yang & Blake, [2012](#)). Consistent with these findings, a study comparing detection of flashed targets presented at different times during the sequence of CFS masks found that detection of the flashed probe was most suppressed for mask temporal frequencies between 5 and 10 Hz (Kaunitz, Fracasso, Skujevskis, & Melcher, [2014](#)). Even lower optimal temporal frequencies (around 1 Hz) were reported by Han, Lunghi, and Alais ([2016](#)), although the masking in that study was realized as a continuous, smooth noise sequence rather than the common flashed Mondrian masks. Together, these studies suggest that the temporal frequency of the masks plays a critical role in determining the effectiveness of CFS, raising questions about the precise relationship between awareness and temporal masking frequency. However, a wide range of temporal frequencies have been used in previous studies of CFS, ranging up to 32 Hz, and sometimes the frequency is not clearly specified (for a review, see Moors, Stein, Wagemans, & van Ee, [2015](#); Zhu et al., [2016](#)).

One largely unexplored issue is whether temporal factors might interact with the spatial properties of the CFS masks used. This is difficult to ascertain because across studies, the exact design of the CFS masks varies widely (e.g., Moors et al., [2015](#)). Due to the multitude of different experimental setups, stimuli, and paradigms, a metacomparison of suppression depth does not seem feasible. Despite being somewhat similar overall in being made up of colored patches, Mondrian masks may vary widely in spatial density, luminance, and color contrast.

More generally, the role of temporal factors in CFS is important for debates regarding the nature of “unconscious processing.” Many studies using CFS compare performance for detecting or discriminating stimuli that differ on a particular property, such as upright versus inverted faces (Stein, Reeder, & Peelen, [2016](#); Stein, Sterzer, & Peelen, [2012](#)). One assumption implicit in these studies is that any feature which influences performance even for “invisible” stimuli must involve a specific computation that can occur even without awareness (Dijksterhuis & Aarts, [2003](#); Gaillard et al., [2006](#); Kaunitz, Fracasso, Lingnau, & Melcher, [2013](#)). Given the hierarchical nature of visual processing, one potential explanation is that features that are processed relatively quickly are less disrupted by CFS, while conscious object formation, which may take up to 150–200 ms (for review, see Wutz & Melcher, [2014](#)), is reset by the flash of a new stimulus. In support for this idea, detection under CFS improves for targets presented for longer durations, reaching plateau at around 100–150 ms (Kaunitz et al., [2014](#)). Thus, one interpretation of unconscious processing of CFS is that it is most likely to occur for features that are processed quickly, and less probable for stimulus features that require longer temporal integration periods or for processes that involve extensive feedback from higher level areas.

As described already, the exact nature by which CFS prevents the target stimulus from reaching conscious awareness is still unknown. We have theorized that the more demanding the flashed masks are in terms of visual processing, the more processing resources they may capture over a longer period of time, resulting in reduced availability of resources for the target stimulus.

Here we endeavor to investigate the effect of two important spatial factors in Mondrian masks for CFS, to improve understanding of how CFS functions but also to illustrate the need for better methodological documentation in future studies. First, we investigate the role of spatial density on masking effectiveness as measured by suppression duration. In many studies, the masks used are of Mondrian-like design but lack precise descriptions regarding spatial density or general design parameters. Of the multitude of possibly involved visual subsystems, we specifically targeted the edge-detection and segmentation circuitry. Edge detection and segmentation happen early in the visual-processing hierarchy (Hubel & Wiesel, [1959](#), [1968](#)) and can be challenged in a controlled way by adding or subtracting mask edges. If indeed a reduced number of edges leads to reduced mask effectiveness (i.e., suppression

duration), then we would expect this deficit to be resultant from either the reduced contrast energy in each mask or the reduced workload imposed on the edge-detection and segmentation circuitry of the visual brain. In the latter case, an increase in the temporal frequency of the mask presentations may be able to increase the workload and recover at least some of the deficit. In this case, we would still expect a reduction in mask effectiveness, but coupled with an upward shift of the optimal temporal masking frequency (see [Figure 1](#)).

## Figure 1



[View Original](#) [Download Slide](#)

Hypothesized shift of mask effectiveness. Black: original masks. Blue: mask effectiveness reduced. Red: mask effectiveness reduced, but partially recovered with an upward shift of the optimal temporal frequency.

Second, we investigated whether the presence of color in the masks affects suppression effectiveness, and if there may be an interaction between the presence of color and the most effective masking frequency. This parameter also varies between studies, and precise descriptions of the number of colors (respectively, gray levels) per mask are frequently lacking. The removal of color may reduce the workload on the visual system, resulting in reduced mask effectiveness. Hence, we theorized that masks without color might be processed faster than their colorful counterparts, and may thus need higher temporal frequencies to absorb the same amount of processing resources in order to achieve the same suppression duration. Alternatively, the removal of color may simply reduce the general saliency of the masks, reducing mask effectiveness without affecting the optimal temporal frequency.

## Ethics statement

The experiment was approved by the ethics committee of the University of Trento, and performed according to the principles expressed in the Declaration of Helsinki. Written informed consent was obtained from all participants.

# Methods

## Apparatus

Visual stimulation was presented on a 21-in. Mitsubishi CRT monitor (1,024 × 768 pixel resolution, 160-Hz frame rate). Subjects viewed the presentation through a mirror stereoscope, with their heads stabilized by a chin-and-head rest. The physical viewing distance was 57 cm, while the optical distance was increased by approximately 9.5 cm due to the detour through the mirror stereoscope. To achieve good fusion of the display, the spatial distance between the left and right presentation areas as well as the angle of the mirrors were adjusted for each observer. Visual stimuli were presented in MATLAB (The MathWorks, Inc., Natick, MA) using the Psychophysics Toolbox (Brainard, [1997](#)).

## Stimuli and masks

### Target stimuli

The stimuli used in the experiment were photographic face and house images (160 each) that were previously used by Zhu et al. ([2016](#)). The images were converted from RGB color to grayscale using MATLAB built-in `rgb2gray` routine, which is a simple linear combination of the RGB color channels ( $0.2989 \times R + 0.5870 \times G + 0.1140 \times B$ ). The luminance histograms of the images were equated by using the SHINE toolbox to minimize potential low-level confounds in our study (Willenbockel et al., [2010](#)).

Examples of the resulting stimulus images are shown in [Figure 2](#). The stimulus images were cropped into a rectangular shape extending  $6.8^\circ \times 8.5^\circ$  and blended into the medium-gray background with a soft oval edge. These images were chosen because they are proven to cause reliable differences in break-through CFS conditions (Zhu et al., [2016](#)), which enables us to verify that our subjects are following the task instructions (see later) rather than just randomly pushing buttons.

## Figure 2



[View Original](#) [Download Slide](#)

Sample stimuli. To comply with copyright requirements, the original face stimuli were replaced with stand-ins that were preprocessed in an identical fashion and match the

visual appearance of the actual stimuli. All images are copyright of the authors where applicable.

## Mask stimuli

While Mondrian's paintings were the result of careful study and planning (Jaffé, [1956/1986](#)), Mondrian masks typically involve a randomization process that combines different, overlapping rectangles. Here, we define in detail the design of the masks used in this study, an overview of which can be seen in [Figure 3](#). For each type, 200 individual masks were generated.

## Figure 3



[View Original](#) [Download Slide](#)

Two samples of each mask type, ordered left to right by decreasing spatial density.

### Normal Mondrian masks

Samples of all mask types used can be seen in [Figure 3](#). The masks used in this study (see also Zhu et al., [2016](#)) were created by a computer algorithm, starting with a white rectangle of  $8.5^\circ \times 10.6^\circ$ , onto which a sequence of 1,000 rectangles of random size, color, and position was then painted. Individual rectangles were sized between  $0.12^\circ$  and  $1.2^\circ$  visual field, with horizontal and vertical size randomized independently. Colors were randomly chosen from RGBCMYKW, as these are all the possible colors when allowing only zero or the available maximum as the RGB intensities of each color. This way, any two colors of the chosen palette have at least one color channel differing at maximum, which should ensure good contrast between colors in terms of both chroma and luminance.

These parameters used in mask creation were chosen in an attempt to create masks that are of repeatable, random construction but visually similar to CFS masks used in other studies.

### Reduced-density masks

In order to evaluate the effect that the spatial density (the number of colorful patches

per mask) might have on mask effectiveness, we created reduced-density masks by magnifying the center region of the normal masks to 200%, 400%, and 800%, resulting in masks with respective densities of 50%, 25%, and 12.5% relative to the original masks.

We determined the size of the average patch on each mask type by means of a scan-line length analysis. For each horizontal line and vertical column of pixels of each mask, we measured the average length before a change of color occurred. All measured lengths across all masks were then pooled into histograms, as shown in [Figure 4A](#). For Mondrian-type masks as the ones used here, the composition of the spatial-frequency spectrum results from the edges between colored patches. As magnifying and cropping a mask by a certain factor inevitably reduces the total number of edges by the same factor, a corresponding reduction of average amplitudes in the Fourier spectrum results (see [Figure 4B](#)). As is to be expected from the rectangular, rigid design of the masks, most of the Fourier energy resides on the cardinal axes of the spectrum, corresponding to horizontal and vertical orientations. However, the reduction of energy following the reduced number of edges in the lower-density masks is also found on the oblique angles of the spectrum, as shown in [Figure 5](#), even though the amplitudes here are substantially reduced compared to the cardinal angles, as can also be seen from [Figure 4B](#).

## Figure 4



[View Original](#) [Download Slide](#)

Mask statistics. (A) Patch-size distribution across different mask types. Data obtained by means of a scan-line length analysis. Values in the top right corner give average patch size across bins. (B) Mean amplitude spectra of mask types, corresponding to (A).

## Figure 5



[View Original](#) [Download Slide](#)

Fourier amplitude comparison along cardinal and oblique directions of the spectrum, averaged across 200 masks each. (A) Spectral amplitude per mask type. (B) Relative change in spectral energy when mask density is reduced (separate for each step—original to 50%, etc.).

### Pixel-noise masks

These masks were made up of color patches (still chosen from the same eight colors), with the color randomly selected for each pixel. The maximum density a computer display is capable of is achieved by setting a different random color for every pixel. While this represents the maximum possible density, it is likely that the resolution capacity of the observer's eye will be exceeded, resulting in spatial averaging that reduces the effective density and contrast of the masks.

### Flat-color masks

By design the opposite of the pixel-noise masks, these masks are of a single random color and have no spatial structure.

## Experiment 1

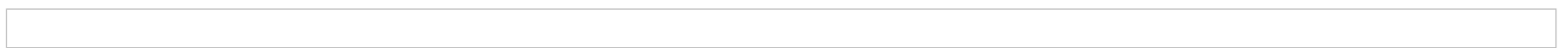
In the first experiment, we evaluated the CFS effectiveness of six different mask types that were designed to vary primarily by spatial density. We tested the hypothesis that more spatially dense masks might require more processing resources, over a longer time period, and thus shift the optimal temporal frequency toward a slower one. Conversely, we hypothesized that less dense masks would require faster temporal refresh rates in order to be as effective in masking.

### Experimental paradigm

Every subject completed six sessions of two blocks each, with one mask type per session. The order of mask types was randomized across subjects. In each block there were 80 face trials, 80 house trials, and 32 empty (no target stimulus) catch trials. All of the images were presented in random order, and only once per session for each subject. House, face, and catch trials were also balanced across masking frequencies. As in our previous study (Zhu et al., [2016](#)), 10 masking frequencies were used: 0, 1, 3, 5, 7, 10, 13, 16, 20, and 32 Hz. All frequencies occurred equally often in each block. A total of 200 trials were collected in each block, with 16 target-present trials and four catch trials per frequency, resulting in a total of 2,400 trials per subject.

In a break-through CFS paradigm, the masks were flashed to the dominant eye at predefined frequencies while the target stimulus image was presented to the other eye (Figure 6). The presentation size of the masks was  $8.5^\circ \times 10.6^\circ$ . Two static frames ( $10.2^\circ \times 12.6^\circ$ ) surrounded the outer border of target stimuli and masks presented on the two sides of the screen, such that both frames were visible only to their respective corresponding eye. Prior to the first trial of each block, the mirror setup and the distance between the two surrounding frames were adjusted individually for each subject, to allow good fusion between both frames. Each trial started with a central fixation cross extending  $1^\circ$  shown for a random period between 800 and 1,000 ms. Masks were then flashed for a random period between 1,500 and 2,000 ms before the target stimulus began to ramp up to the other eye. The contrast of the stimulus image increased from 0% to 100% linearly in 6 s (around 0.1% per display refresh with 8-bit precision), while the repetitive mask display to the dominant eye continued. Subjects were instructed to press the space button as quickly as possible when they saw any part of the target image, but not before they could see the target (break-through CFS). Subjects were informed that there could be catch trials without a target, on which no response was to be given. Images disappeared after subjects pressed the button, or after the trial timed out once full contrast was reached (6 s).

## Figure 6



[View Original](#) [Download Slide](#)

Experimental paradigm (break-through CFS). The contrast of the stimulus images increased continuously from 0% to 100% over a period of 6 s. Subjects were instructed to press the space bar as quickly as possible when they saw an image. By this design, the measured break-through contrast was equivalent to the response time or duration of suppression.

## Analysis

As a measure of central tendency, the mean of the break-through contrast of each masking frequency and each mask type was computed per subject on log-transformed data. In order to identify the optimal masking frequency at a finer scale, a skewed,

raised Gaussian function was fitted to the measured break-through contrast (starting at 3 Hz), and the location of the peak in the fitted function was determined. To test for statistically significant differences between peak frequencies, a hybrid bootstrap procedure was applied. Random sets of subjects were drawn ( $N = 15$ , with replacement), and the fitting procedure was then performed on the random set. In every repetition ( $N = 10,000$ ), the peak frequency of the resulting fit was calculated. Finally, the bootstrapped peak frequencies of the compared conditions were subtracted from each other, and a sign test (two-tailed) was performed on the result. For other comparisons, as indicated, the break-through contrast (determined as the percentage of contrast at the time when the subject pressed the button) was analyzed by an ANOVA design for repeated measures with the masking frequency (10 different frequencies), mask type (6 levels), and stimulus type (faces vs. houses) as within-subject factors. Greenhouse–Geisser adjustments to the degrees of freedom were applied when appropriate and are reported in subscript.

## Subjects

A group of 15 subjects participated in the experiment (14 women, one man; aged 19–29 years,  $M = 23$ ,  $SD = 2.9$ ). The participants were students or postdoctoral fellows recruited from the University of Trento and were paid for their participation. All participants reported normal or corrected-to-normal vision and were unaware of the purpose of the experiment. Ocular dominance was determined by an ABC test (Miles, [1929](#), [1930](#)).

## Results

Replicating previous results (Zhu et al., [2016](#)), for the normal mask the break-through contrast differed significantly between temporal masking frequencies,  $F(9_{2.311}, 126_{32.45}) = 15.079$ ,  $p < 0.001$ . The same held for all reduced-density masks and the pixel-noise masks, but not for the flat-color masks—50% density:  $F(9_{2.464}, 126_{34.54}) = 12.711$ ,  $p < 0.001$ ; 25% density:  $F(9_{1.949}, 126_{27.28}) = 12.52$ ,  $p < 0.001$ ; 12.5% density:  $F(9_{1.932}, 126_{27.05}) = 15.75$ ,  $p < 0.001$ ; pixel-noise:  $F(9_{3.02}, 126_{42.21}) = 11.42$ ,  $p < 0.001$ ; flat-color:  $F(9_{3.20}, 126_{44.86}) = 0.89$ ,  $p = 0.54$ . Significant differences in average break-through contrast were also found between the different mask types,  $F(5_{1.44}, 70_{20.17}) = 20.20$ ,  $p < 0.001$ , even though all mask types appeared to follow the same overall trend, with the lowest break-through contrast at either 0 or 32 Hz and a maximum in between 3 and 20 Hz

(see [Figure 7A](#)). The highest overall break-through contrast was found with the normal masks (maximum of 29% contrast, equaling 1.75 s), with contrast decreasing in step with mask density for the reduced-density masks (26.5% = 1.59 s, 25% = 1.50 s, and 19.5% = 1.18 s). Pixel-noise masks resulted in even lower overall break-through contrast (15% = 0.90 s), and the lowest suppression effectiveness was found with the flat-color masks (12.5% = 0.74 s).

## Figure 7

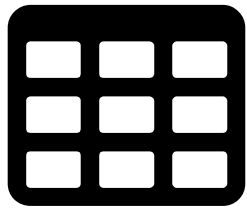


[View Original](#) [Download Slide](#)

Main results. (A) Break-through duration/contrast over 10 temporal frequencies; colors indicate mask types. Mean and standard error of the mean are across subjects. Thick lines represent measured data, thin lines represent the fitted function, and black markers represent the location of the peak frequency as determined by function fitting. (B) Pairwise hybrid test results between peak frequencies of different mask types. Any pairs connected by blue bars differ significantly (see also [Table 1](#)).

We analyzed the relationship between density and temporal frequency in two ways. First, we measured the peak suppression frequencies, as determined by fitting a skewed Gaussian to the data. This peak suppression frequency inversely followed the spatial density of the masks: The lowest peak frequency resulted from the pixel-noise masks, and the highest from the flat-color masks (although the quality of fit with the flat-color masks is questionable due to the overall rather flat profile of the measured results). The statistical results of the pairwise comparisons of peak masking frequency can be found in [Table 1](#) and [Figure 7B](#). The flat-color masks were excluded from the statistical tests, as the fitting of the peak frequency was unreliable due to their very weakly expressed peak characteristics of suppression—only with the flat-color masks does the standard error exceed the distance between the minimum and maximum of the measured curve. The break-through contrast also differed significantly between the different target stimuli (faces vs. houses),  $F(1, 14) = 23.29, p < 0.001$ , again replicating the results reported by Zhu et al. (2016). Subjects responded rarely on catch trials (average = 4.6%,  $SD = 5.9\%$ , maximum = 25.4%), indicating good compliance with the instructions given.

# Table 1



[View Table](#)

Pairwise statistical comparisons of peak suppression frequency between mask types (Bonferroni–Holm corrected). Significant results are emphasized.

---

Further scrutinizing the relationship between peak masking frequency and mask spatial density, we correlated the spatial density of the mask type with the associated peak temporal frequency ([Figure 8](#)). In the presence of noise, the fitting procedure can sometimes fail to achieve a good quality of fit for individual subjects. In the case of the 12.5% density stimuli, the peak in the suppression characteristic is also expressed only weakly, which, again in the presence of noise, causes less reliable fits—this explains the increase in variance between the individual data points. We therefore excluded those data points from the correlation analysis where the peak frequency resulting from the fitting procedure was below 1 Hz or above 30 Hz. The normal, 50% density, 25% density, and 12.5% density masks were included in the analysis. The correlation between decreasing spatial density and increasing temporal frequency was significant (Pearson:  $R = -0.94$ ,  $p = 0.030$ ; Spearman:  $R = -1$ ,  $p = 0.042$ ; one-tailed).

## Figure 8



[View Original](#) [Download Slide](#)

Correlation between spectral density and optimal temporal frequency. Bar graphs represent mean and standard error of the mean for peak frequency across subjects.

In a second analysis, we investigated whether the shift in peak influenced the suppression effectiveness of the theta-frequency (5–7 Hz) Mondrian mask. As shown in [Figure 7](#), the break-through time/contrast at 6 Hz was similar to the peak suppression contrast. Thus, the main effect of reducing density was to extend the range of the peak

suppression effect, reducing the temporal tuning of the function. It is interesting to note that for all of the Mondrian masks, performance converged to a similar value at 32 Hz, while for the pixel-noise and flat-color masks, break-through time/contrast converged at a much lower value (around 700 ms or 12% contrast, rather than 1,200 ms or 20% contrast). One possible interpretation is that this reflects the involvement of two processes, one requiring flashing of CFS masks at a theta to alpha frequency (perhaps involving the parvocellular and high-spatial-frequency, low-temporal-frequency visual system) and the other (present even for the 32-Hz displays) more reflecting the contribution of the magnocellular system (Han et al., [2016](#)).

## Experiment 2

In the second experiment, we tested masks of two different spatial densities (normal and 25% density) in either full color or grayscale. We tested the hypothesis that the removal of color, which is thought to be processed more slowly than luminance, might require greater temporal frequencies in order to reach peak suppression. We also tested whether removing color might only diminish the image saliency, leading to less effective masks in general but the same peak temporal frequency range.

## Subjects

A second group of 16 subjects was recruited for the second experiment (eight women, eight men; aged 19–29 years,  $M = 23$ ,  $SD = 2.9$ ).

## Methods and analysis

The focus of the second experiment was on a comparison of colored masks and their grayscale counterparts. From [Experiment 1](#), the normal masks and the 25% density masks were selected, as they showed the overall longest suppression durations while having significantly different peak frequencies. This also allowed us to replicate the main finding of the first experiment (faster temporal frequency required for less dense masks) in a second set of participants. Grayscale masks were generated from the colored masks by use of MATLAB's built-in `rgb2gray` function (see Target stimuli, earlier), turning the eight colors (RGBCMYKW) into six distinct shades of gray plus white and black. While the experimental paradigm was unchanged from [Experiment 1](#) aside from the masks used, the setup was calibrated for linear luminance on all three RGB channels to avoid introducing unintentional bias from the grayscale conversion. Using

a Minolta CS100A photometer, eight luminance intensities distributed evenly across the monitor's luminance range were measured for each RGB channel separately. A compensation function for each RGB channel was then interpolated from these measurements and applied to the display code. The procedure ensured that whites and blacks in the grayscale masks were identical to the whites and blacks of the color masks, with even distribution of the gray levels in between. Absolute luminance contrast for both color and gray masks was therefore identical.

Analysis steps were performed analogously to [Experiment 1](#).

## Results

[Figure 9](#) shows the general results of [Experiment 2](#). First, the color versions of the masks replicated the results from [Experiment 1](#), with the higher density masks most effective at a slower temporal frequency than the less dense masks. In addition, the grayscale versions of both the normal and the reduced-density masks proved to be less effective than their respective color versions—normal:  $F(1, 15) = 29.62, p < 0.001$ ; 25% density:  $F(1, 15) = 37.36, p < 0.001$ ; however, the general frequency profile remained very similar after removal of color, and the differences in peak frequency were not significant for either the normal masks ( $p = 0.91$ ) or the reduced-density masks ( $p = 0.50$ ). Color masks achieved a maximum suppression of 31%, equaling 1.87 s, and 20%, equaling 1.20 s (normal vs. 25% density); gray masks achieved 27.8%, equaling 1.67 s, and 16.5%, equaling 0.99 s. Catch-trial analysis again revealed good compliance with the instructions given (average = 2.0%,  $SD = 2.2\%$ , maximum = 9.2%).

## Figure 9



[View Original](#) [Download Slide](#)

Color versus gray: Comparison between color and grayscale versions of two mask types (normal and 25% density). Thick lines represent measured data, thin lines represent the fitted function, and black markers represent the location of the peak frequency as determined by function fitting.

## Discussion

The main finding of this study was that mask density, but not color, influenced the relationship between the temporal frequency of the mask and CFS effectiveness. We replicated previous findings that the optimal frequency for CFS appears to be around 6 Hz (Tsuchiya & Koch, [2005](#); Zhu et al., [2016](#)). However, we also showed that this relationship depends on the stimulus density, which was related to the average size and number of patches (and the Fourier amplitude along the cardinal and oblique directions of the spectrum). This finding is consistent with the hypothesis that with less dense images, which would presumably require fewer processing resources over a shorter amount of time, faster temporal frequencies would be useful to mask the target. In contrast, removing color from the masks reduced suppression effectiveness but did not affect the optimal temporal frequency.

What determines the optimal temporal frequency for any type of mask? It is interesting to note that the most effective masking frequency across the various mask types was around 6 Hz (the original masks, [Figure 7A](#)), in the high-theta to low-alpha range. This frequency range has been implicated in detection of near-threshold stimuli (particularly oscillations in the alpha range: Busch, Dubois, & VanRullen, [2009](#); Mathewson, Beck, Fabiani, Ro, & Gratton, [2011](#); VanRullen, Busch, Drewes, & Dubois, [2011](#)), in oscillations in spatial attention (low alpha or high theta: Fiebelkorn et al., [2011](#); Fiebelkorn, Saalmann, & Kastner, [2013](#); Landau & Fries, [2012](#); Song, Meng, Chen, Zhou, & Luo, [2014](#)), and in recurrent processing (theta: Drewes, Zhu, Wutz, & Melcher, [2015](#); Wutz & Melcher, [2014](#); Wutz, Muschter, van Koningsbruggen, & Melcher, [2014](#); Wutz, Weisz, Braun, & Melcher, [2014](#)). On the one hand, theta (5–7 Hz) has been implicated in many tasks involving image categorization or binding features to specific objects or locations (Drewes et al., [2015](#); Wutz, Weisz, et al., [2014](#); Wutz & Melcher, [2014](#)). Higher frequencies, in the alpha band, have been implicated in the temporal resolution of perception (Cecere, Rees, & Romei, [2015](#); Cravo et al., [2015](#); Gho & Varela, [1988](#); Milton & Pleydell, [2016](#); Samaha & Postle, [2015](#); Varela et al., [1981](#)). In between these two ranges, 7–8 Hz has been frequently implicated in studies of the temporal frequency of attention (Dugué, Marque, & VanRullen, [2015](#); Dugué, McLelland, Lajous, & VanRullen, [2015](#); Landau & Fries, [2012](#); Song et al., [2014](#)).

The finding that CFS effectiveness peaks between 5 and 10 Hz also speaks to current findings regarding theories of perceptual cycles (for review, see VanRullen, [2016](#); VanRullen & Koch, [2003](#)). There is accumulating evidence for one or more key

temporal cycles in visual processing, described in terms of perceptual cycles, attentional sampling (Busch & VanRullen, [2010](#); Fiebelkorn et al., [2013](#); Landau & Fries, [2012](#)), or temporal integration windows (Cecere et al., [2015](#); Samaha & Postle, [2015](#)), and these have repeatedly been reported to be in the range of around 5–10 Hz. It has also been suggested that, for example, in the case of the flash-lag illusion, conscious updating is a rhythmic process with a temporal frequency in the range of 5–10 Hz (Chakravarthi & VanRullen, [2012](#)). Thus, CFS might interact with this visual sampling frequency.

In order to optimally disrupt this process prior to the stimulus being fully processed and made available for awareness, the temporal frequency of the mask should be slightly faster than the perceptual cycle. This would suggest that perceptual cycles operating in the theta range would require masks flashing with at least the same frequency to optimally interrupt each cycle before it can be completed. In principle, more masks in each cycle would then increase the chance for successful interruption, implying that the higher the masking frequency, the more effective the masking should become.

In the current study, peak suppression was consistently found at around 6 Hz, with more dense displays showing a rapid drop-off in suppression effectiveness but more sparse Mondrian patterns yielding a slower decay in effectiveness. In both studies, performance with Mondrian masks converged to a similar value at 32 Hz. As described already, this may indicate the involvement of two processes. Consistent with the suggestion of Han et al. ([2016](#)), the lower-temporal-frequency, high-spatial-frequency masks might preferentially activate the parvocellular system, while the high-temporal-frequency and low-spatial-frequency stimulation (32-Hz displays) may show the contribution of the magnocellular system.

Alternatively, entrainment of a forced rhythm close to the frequency of the perceptual moments might interfere with perceptual sampling at an early level. However, the peak suppression frequency found here covers more than two octaves as mask density is reduced, which would imply that the frequency of the perceptual cycles would shift by a similar amount. Such a high range of frequency entrainment seems unlikely. In addition, as it is generally not obvious how the density of the masks would affect the frequency of the perceptual cycles, we would rather expect a mostly

constant peak frequency if entrainment of a forced rhythm were the underlying cause of suppression. We found, instead, a variable rather than a constant optimal frequency, which makes entrainment seem unlikely as the main mechanism of suppression.

Another possibility is that CFS might suppress awareness of the target by repeatedly biasing competition toward the highly salient mask within the same level of visual processing, as in traditional binocular rivalry (Alais & Melcher, [2007](#); Han et al., [2016](#); Tong, Meng, & Blake, [2006](#)), before target processing can be completed. This may also explain the effectiveness of the continuous, low-temporal-frequency (nonflashing) noise used by Han et al. ([2016](#)). Those authors further proposed a particular involvement of the parvocellular network, which is known to be most sensitive to high spatial and low temporal frequency. Color is also one of the features processed mainly in the parvocellular network (Ungerleider & Mishkin, [1982](#)). In principle, this may explain the reduced suppressive power found when we removed color from our masks ([Experiment 2](#)). However, if the removal of color changed the balance of involvement between the parvocellular (slow) and magnocellular (fast) networks, we would have expected a change also in the peak suppressive frequency (toward faster rates). However, no such change was found, which means that either the magnocellular network plays no significant role in CFS or the mechanism is in fact more complicated than assumed in this thought. A simpler explanation would be that the removal of color simply reduced the overall saliency or effective contrast of the masks, as there are indications that color may not be processed exclusively in the parvocellular pathway (Claeys et al., [2004](#)).

A change in balance between magno- and parvocellular pathways may, however, be an alternate explanation of the shift in preferred frequency and the generally reduced suppression effectiveness with lower spatial mask densities. As seen from [Figure 5B](#), when mask density is reduced, Fourier energy is shifted away from high spatial frequencies and toward lower spatial frequencies, contrary to the preference of the parvocellular pathway. This may result in a lesser impact on the parvocellular (slow) pathway and a higher impact on the magnocellular (fast) pathway, requiring higher temporal frequencies for optimal effectiveness.

A further possibility underlying CFS would be interference with the process which

allows target-related information to be widely transmitted to other brain regions (e.g., Global Workspace Model: Dehaene, Kerszberg, & Changeux, [1998](#); Newman, Baars, & Cho, [1997](#)).

However, there are likely other factors playing a role in CFS masking. An additional limiting factor to the improvement in mask effectiveness with higher temporal frequencies may be flicker fusion. While critical (absolute) flicker fusion (the point where a flickering patch gives the same perceptual impression as a patch of constant brightness) is generally reported at higher frequencies than tested in the current study (Brindley, Du Croz, & Rushton, [1966](#); Capilla & Aguilar, [1993](#)), perceived contrast can already be significantly reduced at much lower frequencies. Increasing the temporal frequency of the mask display may therefore reduce the effective contrast of the masks, in turn reducing masking effectiveness. The point of optimal suppression effectiveness would then be the intersection between the two curves describing the increased chance to interrupt ongoing processing and the reduced effective contrast due to flicker fusion.

In terms of methodological implications, the current findings once more point out that the 10-Hz masking frequency used in most current CFS studies may not be optimally effective. Moreover, optimal frequency and mask density interact, highlighting the need for accurate and detailed description of CFS mask design in order to achieve better comparability across studies. Otherwise, our findings suggest that the range of spatial and temporal parameters that have been used in previous studies would tend to lead to inconsistent and possibly contradictory findings.

## Acknowledgments

JD and DM were supported by a European Research Council grant (Grant Agreement No. 313658) and High-level Foreign Expert Grant (GDT20155300084).

We would like to thank Maddalena Costanzo for her help with data collection.

Commercial relationships: none.

Corresponding authors: Jan Drewes; Weina Zhu.

Email: [mail@jandrewes.de](mailto:mail@jandrewes.de); [zhuweina.cn@gmail.com](mailto:zhuweina.cn@gmail.com).

Address: Center for Mind/Brain Sciences (CIMEC), University of Trento, Rovereto, Italy;  
School of Information Science, Yunnan University, Kunming, China.

## References

- Alais, D., & Melcher, D. (2007). Strength and coherence of binocular rivalry depends on shared stimulus complexity. *Vision Research*, 47 (2), 269–279, doi:[10.1016/j.visres.2006.09.003](https://doi.org/10.1016/j.visres.2006.09.003).
- Brainard, D. H. (1997). The Psychophysics Toolbox. *Spatial Vision*, 10, 433–436.
- Brindley, G. S., Du Croz, J. J., & Rushton, W. A. H. (1966). The flicker fusion frequency of the blue-sensitive mechanism of colour vision. *The Journal of Physiology*, 183 (2), 497–500.
- Busch, N. A., Dubois, J., & VanRullen, R. (2009). The phase of ongoing EEG oscillations predicts visual perception. *The Journal of Neuroscience*, 29 (24), 7869–7876, doi:[10.1523/JNEUROSCI.0113-09.2009](https://doi.org/10.1523/JNEUROSCI.0113-09.2009).
- Busch, N. A., & VanRullen, R. (2010). Spontaneous EEG oscillations reveal periodic sampling of visual attention. *Proceedings of the National Academy of Sciences, USA*, 107 (37), 16048–16053, doi:[10.1073/pnas.1004801107](https://doi.org/10.1073/pnas.1004801107).
- Capilla, P., & Aguilar, M. (1993). Red-green flicker resolution as a function of heterochromatic luminous modulation. *Ophthalmic & Physiological Optics*, 13 (2), 183–185.
- Cecere, R., Rees, G., & Romei, V. (2015). Individual differences in alpha frequency drive crossmodal illusory perception. *Current Biology*, 25 (2), 231–235, doi:[10.1016/j.cub.2014.11.034](https://doi.org/10.1016/j.cub.2014.11.034).
- Chakravarthi, R., & VanRullen, R. (2012). Conscious updating is a rhythmic process. *Proceedings of the National Academy of Sciences, USA*, 109 (26), 10599–10604, doi:[10.1073/pnas.1121622109](https://doi.org/10.1073/pnas.1121622109).
- Claeys, K. G., Dupont, P., Cornette, L., Sunaert, S., Van Hecke, P., De Schutter, E., & Orban, G. A. (2004). Color discrimination involves ventral and dorsal stream visual areas. *Cerebral Cortex*, 14 (7), 803–822, doi:[10.1093/cercor/bhh040](https://doi.org/10.1093/cercor/bhh040).
- Costello, P., Jiang, Y., Baartman, B., McGlennen, K., & He, S. (2009). Semantic and subword priming during binocular suppression. *Consciousness and Cognition*, 18 (2), 375–382, doi:[10.1016/j.concog.2009.02.003](https://doi.org/10.1016/j.concog.2009.02.003).
- Cravo, A. M., Santos, K. M., Reyes, M. B., Caetano, M. S., & Claessens, P. M. E. (2015). Visual causality judgments correlate with the phase of alpha oscillations. *Journal of Cognitive Neuroscience*, 27 (10), 1887–1894, [https://doi.org/10.1162/jocn\\_a\\_00832](https://doi.org/10.1162/jocn_a_00832).
- Dehaene, S., Kerszberg, M., & Changeux, J. P. (1998). A neuronal model of a global workspace in effortful cognitive tasks. *Proceedings of the National Academy of Sciences, USA*, 95 (24), 14529–14534.
- Dijksterhuis, A., & Aarts, H. (2003). On wildebeests and humans: The preferential detection of

negative stimuli. *Psychological Science*, 14 (1), 14–18.

Drewes, J., Zhu, W., Wutz, A., & Melcher, D. (2015). Dense sampling reveals behavioral oscillations in rapid visual categorization. *Scientific Reports*, 5, 16290, doi:[10.1038/srep16290](https://doi.org/10.1038/srep16290).

Dugué, L., Marque, P., & VanRullen, R. (2015). Theta oscillations modulate attentional search performance periodically. *Journal of Cognitive Neuroscience*, 27 (5), 945–958, doi:[10.1162/jocn\\_a\\_00755](https://doi.org/10.1162/jocn_a_00755).

Dugué, L., McLelland, D., Lajous, M., & VanRullen, R. (2015). Attention searches nonuniformly in space and in time. *Proceedings of the National Academy of Sciences, USA*, 112 (49), 15214–15219, doi:[10.1073/pnas.1511331112](https://doi.org/10.1073/pnas.1511331112).

Fiebelkorn, I. C., Foxe, J. J., Butler, J. S., Mercier, M. R., Snyder, A. C., & Molholm, S. (2011). Ready, set, reset: Stimulus-locked periodicity in behavioral performance demonstrates the consequences of cross-sensory phase reset. *The Journal of Neuroscience*, 31 (27), 9971–9981, doi:[10.1523/JNEUROSCI.1338-11.2011](https://doi.org/10.1523/JNEUROSCI.1338-11.2011).

Fiebelkorn, I. C., Saalmann, Y. B., & Kastner, S. (2013). Rhythmic sampling within and between objects despite sustained attention at a cued location. *Current Biology*, 23 (24), 2553–2558, doi:[10.1016/j.cub.2013.10.063](https://doi.org/10.1016/j.cub.2013.10.063).

Gaillard, R., Del Cul, A., Naccache, L., Vinckier, F., Cohen, L., & Dehaene, S. (2006). Nonconscious semantic processing of emotional words modulates conscious access. *Proceedings of the National Academy of Sciences, USA*, 103 (19), 7524–7529, doi:[10.1073/pnas.0600584103](https://doi.org/10.1073/pnas.0600584103).

Gho, M., & Varela, F. J. (1988–1989). A quantitative assessment of the dependency of the visual temporal frame upon the cortical rhythm. *Journal De Physiologie*, 83 (2), 95–101.

Han, S., Lunghi, C., & Alais, D. (2016). The temporal frequency tuning of continuous flash suppression reveals peak suppression at very low frequencies. *Scientific Reports*, 6, 35723, doi:[10.1038/srep35723](https://doi.org/10.1038/srep35723).

Hubel, D. H., & Wiesel, T. N. (1959). Receptive fields of single neurones in the cat's striate cortex. *The Journal of Physiology*, 148, 574–591.

Hubel, D. H., & Wiesel, T. N. (1968). Receptive fields and functional architecture of monkey striate cortex. *The Journal of Physiology*, 195 (1), 215–243.

Jaffé, H. L. C. (1986). *De Stijl: 1917–1931. The Dutch contribution to modern art*. Amsterdam: Meulenhoff/Landshoff. (Original work published 1956)

Jiang, Y., Costello, P., & He, S. (2007). Processing of invisible stimuli: Advantage of upright faces and recognizable words in overcoming interocular suppression. *Psychological Science*, 18 (4), 349–355, doi:[10.1111/j.1467-9280.2007.01902.x](https://doi.org/10.1111/j.1467-9280.2007.01902.x).

- Jiang, Y., Shannon, R. W., Vizueta, N., Bernat, E. M., Patrick, C. J., & He, S. (2009). Dynamics of processing invisible faces in the brain: Automatic neural encoding of facial expression information. *NeuroImage*, 44 (3), 1171–1177, doi:[10.1016/j.neuroimage.2008.09.038](https://doi.org/10.1016/j.neuroimage.2008.09.038).
- Kang, M.-S., Blake, R., & Woodman, G. F. (2011). Semantic analysis does not occur in the absence of awareness induced by interocular suppression. *The Journal of Neuroscience*, 31 (38), 13535–13545, doi:[10.1523/JNEUROSCI.1691-11.2011](https://doi.org/10.1523/JNEUROSCI.1691-11.2011).
- Kaunitz, L., Fracasso, A., Lingnau, A., & Melcher, D. (2013). Non-conscious processing of motion coherence can boost conscious access. *PLoS ONE*, 8 (4), e60787, doi:[10.1371/journal.pone.0060787](https://doi.org/10.1371/journal.pone.0060787).
- Kaunitz, L., Fracasso, A., & Melcher, D. (2011). Unseen complex motion is modulated by attention and generates a visible aftereffect. *Journal of Vision*, 11 (13): 10, 1–9, doi:[10.1167/11.13.10](https://doi.org/10.1167/11.13.10).  
[PubMed] [Article]
- Kaunitz, L., Fracasso, A., Skujevskis, M., & Melcher, D. (2014). Waves of visibility: Probing the depth of inter-ocular suppression with transient and sustained targets. *Frontiers in Psychology*, 5, doi:[10.3389/fpsyg.2014.00804](https://doi.org/10.3389/fpsyg.2014.00804).
- Landau, A. N., & Fries, P. (2012). Attention samples stimuli rhythmically. *Current Biology*, 22 (11), 1000–1004, doi:[10.1016/j.cub.2012.03.054](https://doi.org/10.1016/j.cub.2012.03.054).
- Levelt, W. J. M. (1965). *On binocular rivalry*. Soesterberg, the Netherlands: Institute for Perception RVO-TNO. Retrieved from [http://www.mpi.nl/world/materials/publications/levelt/Levelt\\_Binocular\\_Rivalry\\_1965.pdf](http://www.mpi.nl/world/materials/publications/levelt/Levelt_Binocular_Rivalry_1965.pdf)
- Lin, Z., & He, S. (2009). Seeing the invisible: The scope and limits of unconscious processing in binocular rivalry. *Progress in Neurobiology*, 87 (4), 195–211, doi:[10.1016/j.pneurobio.2008.09.002](https://doi.org/10.1016/j.pneurobio.2008.09.002).
- Lin, Z., & Murray, S. O. (2014). Unconscious processing of an abstract concept. *Psychological Science*, 25 (1), 296–298, doi:[10.1177/0956797613504964](https://doi.org/10.1177/0956797613504964).
- Mathewson, K. E., Beck, D. M., Fabiani, M., Ro, T., & Gratton, G. (2011). Pulsed out of awareness: EEG alpha oscillations represent a pulsed-inhibition of ongoing cortical processing. *Frontiers in Perception Science*, 2, 99, doi:[10.3389/fpsyg.2011.00099](https://doi.org/10.3389/fpsyg.2011.00099).
- Miles, W. R. (1929). Ocular dominance demonstrated by unconscious sighting. *Journal of Experimental Psychology*, 12 (2), 113–126, doi:[10.1037/h0075694](https://doi.org/10.1037/h0075694).
- Miles, W. R. (1930). Ocular dominance in human adults. *The Journal of General Psychology*, 3 (3), 412–430, doi:[10.1080/00221309.1930.9918218](https://doi.org/10.1080/00221309.1930.9918218).
- Milton, A., & Pleydell-Pearce, C. W. (2016). The phase of pre-stimulus alpha oscillations influences the visual perception of stimulus timing. *NeuroImage*, 133, 53–61, <https://doi.org/10.1016/j.neuroimage.2016.02.065>.

- Mitroff, S. R., & Scholl, B. J. (2005). Forming and updating object representations without awareness: Evidence from motion-induced blindness. *Vision Research*, 45 (8), 961–967, doi:[10.1016/j.visres.2004.09.044](https://doi.org/10.1016/j.visres.2004.09.044).
- Montaser-Kouhsari, L., Moradi, F., Zandvakili, A., & Esteky, H. (2004). Orientation-selective adaptation during motion-induced blindness. *Perception*, 33 (2), 249–254.
- Moors, P., Hesselmann, G., Wagemans, J., & van Ee, R. (2017). Continuous flash suppression: Stimulus fractionation rather than integration. *Trends in Cognitive Sciences*, 0 (0), doi:[10.1016/j.tics.2017.06.005](https://doi.org/10.1016/j.tics.2017.06.005).
- Moors, P., Stein, T., Wagemans, J., & van Ee, R. (2015). Serial correlations in continuous flash suppression. *Neuroscience of Consciousness*, 2015 (1), niv010, 1–10, doi:[10.1093/nc/niv010](https://doi.org/10.1093/nc/niv010).
- Mudrik, L., Breska, A., Lamy, D., & Deouell, L. Y. (2011). Integration without awareness expanding the limits of unconscious processing. *Psychological Science*, 22 (6), 1–7, doi:[10.1177/0956797611408736](https://doi.org/10.1177/0956797611408736).
- Newman, J., Baars, B. J., & Cho, S.-B. (1997). A neural global workspace model for conscious attention. *Neural Networks*, 10 (7), 1195–1206, doi:[10.1016/S0893-6080\(97\)00060-9](https://doi.org/10.1016/S0893-6080(97)00060-9).
- Samaha, J., & Postle, B. R. (2015). The speed of alpha-band oscillations predicts the temporal resolution of visual perception. *Current Biology*, 25 (22), 2985–2990, doi:[10.1016/j.cub.2015.10.007](https://doi.org/10.1016/j.cub.2015.10.007).
- Smith, M. L. (2012). Rapid processing of emotional expressions without conscious awareness. *Cerebral Cortex*, 22 (8), 1748–1760, doi:[10.1093/cercor/bhr250](https://doi.org/10.1093/cercor/bhr250).
- Song, K., Meng, M., Chen, L., Zhou, K., & Luo, H. (2014). Behavioral oscillations in attention: Rhythmic  $\alpha$  pulses mediated through  $\theta$  band. *The Journal of Neuroscience*, 34 (14), 4837–4844, doi:[10.1523/JNEUROSCI.4856-13.2014](https://doi.org/10.1523/JNEUROSCI.4856-13.2014).
- Stein, T., Hebart, M. N., & Sterzer, P. (2011). Breaking continuous flash suppression: A new measure of unconscious processing during interocular suppression? *Frontiers in Human Neuroscience*, 5, 167, 1–17, doi:[10.3389/fnhum.2011.00167](https://doi.org/10.3389/fnhum.2011.00167).
- Stein, T., Reeder, R. R., & Peelen, M. V. (2016). Privileged access to awareness for faces and objects of expertise. *Journal of Experimental Psychology: Human Perception and Performance*, 42 (6), 788–798, doi:[10.1037/xhp0000188](https://doi.org/10.1037/xhp0000188).
- Stein, T., Sterzer, P., & Peelen, M. V. (2012). Privileged detection of conspecifics: Evidence from inversion effects during continuous flash suppression. *Cognition*, 125 (1), 64–79, doi:[10.1016/j.cognition.2012.06.005](https://doi.org/10.1016/j.cognition.2012.06.005).
- Sterzer, P., Stein, T., Ludwig, K., Rothkirch, M., & Hesselmann, G. (2014). Neural processing of visual information under interocular suppression: A critical review. *Frontiers in Psychology*, 5, 453,

doi:[10.3389/fpsyg.2014.00453](https://doi.org/10.3389/fpsyg.2014.00453).

Tong, F., Meng, M., & Blake, R. (2006). Neural bases of binocular rivalry. *Trends in Cognitive Sciences*, 10 (11), 502–511, doi:[10.1016/j.tics.2006.09.003](https://doi.org/10.1016/j.tics.2006.09.003).

Tsuchiya, N., & Koch, C. (2005). Continuous flash suppression reduces negative afterimages. *Nature Neuroscience*, 8 (8), 1096–1101, doi:[10.1038/nn1500](https://doi.org/10.1038/nn1500).

Tsuchiya, N., Koch, C., Gilroy, L. A., & Blake, R. (2006). Depth of interocular suppression associated with continuous flash suppression, flash suppression, and binocular rivalry. *Journal of Vision*, 6 (10): 6, 1068–1078, doi:[10.1167/6.10.6](https://doi.org/10.1167/6.10.6). [PubMed] [Article]

Ungerleider, L. G., & Mishkin, M. (1982). Two cortical visual systems. In Ingle, D. J. Goodale, M. A. & Mansfield R. J. W. (Eds.), *Analysis of visual behavior* (pp. 549–586). Cambridge, MA: MIT Press.

van Boxtel, J. J. A., Tsuchiya, N., & Koch, C. (2010). Opposing effects of attention and consciousness on afterimages. *Proceedings of the National Academy of Sciences, USA*, 107 (19), 8883–8888, doi:[10.1073/pnas.0913292107](https://doi.org/10.1073/pnas.0913292107).

VanRullen, R. (2016). Perceptual cycles. *Trends in Cognitive Sciences*, 20 (10), 723–735, doi:[10.1016/j.tics.2016.07.006](https://doi.org/10.1016/j.tics.2016.07.006).

VanRullen, R., Busch, N., Drewes, J., & Dubois, J. (2011). Ongoing EEG phase as a trial-by-trial predictor of perceptual and attentional variability. *Frontiers in Perception Science*, 2, 60, doi:[10.3389/fpsyg.2011.00060](https://doi.org/10.3389/fpsyg.2011.00060).

VanRullen, R., & Koch, C. (2003). Is perception discrete or continuous? *Trends in Cognitive Sciences*, 7 (5), 207–213.

Varela, F. J., Toro, A., John, E. R., & Schwartz, E. L. (1981). Perceptual framing and cortical alpha rhythm. *Neuropsychologia*, 19 (5), 675–686.

Wheatstone, C. (1838). Contributions to the physiology of vision: Part the first. On some remarkable, and hitherto unobserved, phenomena of binocular vision. *Philosophical Transactions of the Royal Society of London*, 128, 371–394, doi:[10.1098/rstl.1838.0019](https://doi.org/10.1098/rstl.1838.0019).

Willenbockel, V., Javid Sadr, J., Fiset, D., Horne, G. O., Gosselin, F., & Tanaka, J. W. (2010). Controlling low-level image properties: The SHINE toolbox. *Behavior Research Methods*, 42 (3), 671–684, <https://doi.org/10.3758/BRM.42.3.671>.

Wutz, A., & Melcher, D. (2014). The temporal window of individuation limits visual capacity. *Frontiers in Psychology*, 5, 952, doi:[10.3389/fpsyg.2014.00952](https://doi.org/10.3389/fpsyg.2014.00952).

Wutz, A., Muschter, E., van Koningsbruggen, M., & Melcher, D. (2014). Saccades reset temporal integration windows. *Journal of Vision*, 14 (10), 584, <https://doi.org/10.1167/14.10.584>. [Abstract]

Wutz, A., Weisz, N., Braun, C., & Melcher, D. (2014). Temporal windows in visual processing: “Prestimulus brain state” and “poststimulus phase reset” segregate visual transients on different temporal scales. *The Journal of Neuroscience*, 34 (4), 1554–1565, doi:[10.1523/JNEUROSCI.3187-13.2014](https://doi.org/10.1523/JNEUROSCI.3187-13.2014).

Yang, E., & Blake, R. (2012). Deconstructing continuous flash suppression. *Journal of Vision*, 12 (3): 8, 1–14, doi:[10.1167/12.3.8](https://doi.org/10.1167/12.3.8). [[PubMed](#)] [[Article](#)]

Yang, E., Brascamp, J., Kang, M.-S., & Blake, R. (2014). On the use of continuous flash suppression for the study of visual processing outside of awareness. *Frontiers in Psychology*, 5, 724, 1–17, doi:[10.3389/fpsyg.2014.00724](https://doi.org/10.3389/fpsyg.2014.00724).

Zhou, G., Zhang, L., Liu, J., Yang, J., & Qu, Z. (2010). Specificity of face processing without awareness. *Consciousness and Cognition*, 19 (1), 408–412, doi:[10.1016/j.concog.2009.12.009](https://doi.org/10.1016/j.concog.2009.12.009).

Zhu, W., Drewes, J., & Melcher, D. (2016). Time for awareness: The influence of temporal properties of the mask on continuous flash suppression effectiveness. *PLoS ONE*, 11 (7), e0159206, doi:[10.1371/journal.pone.0159206](https://doi.org/10.1371/journal.pone.0159206).

Copyright 2018 The Authors  
This work is licensed under a [Creative Commons Attribution 4.0 International License](https://creativecommons.org/licenses/by/4.0/).

